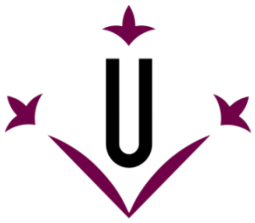

Universitat de Lleida

Document downloaded from:

http://hdl.handle.net/10459.1/69380

The final publication is available at:

https://doi.org/10.1016/j.jfoodeng.2017.03.024

Copyright

cc-by-nc-nd, (c) Elsevier, 2017

Està subjecte a una llicència de
Reconeixement-NoComercial-SenseObraDerivada 3.0 de Creative Commons

Accepted Manuscript

Photo-protection and controlled release of folic acid using edible alginate/chitosan nanolaminates

Acevedo-Fani Alejandra, Soliva-Fortuny Robert, Martín-Belloso Olga

PII:	S0260-8774(17)30119-X
DOI:	10.1016/j.jfoodeng.2017.03.024
Reference:	JFOE 8828
To appear in:	*Journal of Food Engineering*
Received Date:	09 November 2016
Revised Date:	21 March 2017
Accepted Date:	23 March 2017

Please cite this article as: Acevedo-Fani Alejandra, Soliva-Fortuny Robert, Martín-Belloso Olga, Photo-protection and controlled release of folic acid using edible alginate/chitosan nanolaminates, *Journal of Food Engineering* (2017), doi: 10.1016/j.jfoodeng.2017.03.024

This is a PDF file of an unedited manuscript that has been accepted for publication. As a service to our customers we are providing this early version of the manuscript. The manuscript will undergo copyediting, typesetting, and review of the resulting proof before it is published in its final form. Please note that during the production process errors may be discovered which could affect the content, and all legal disclaimers that apply to the journal pertain.

ACCEPTED MANUSCRIPT

Highlights

- Edible folic acid-loaded nanolaminates were successfully developed
- The loading solutions conditions affected the folic acid content in nanolaminates
- Folic acid-loaded nanolaminates were highly stable under UV radiation
- The pH conditions influenced the release profiles of folic acid from nanolaminates

ACCEPTED MANUSCRIPT

ACCEPTED MANUSCRIPT

Photo-protection and controlled release of folic acid using edible alginate/chitosan nanolaminates

Authors:

Acevedo-Fani, Alejandra

Soliva-Fortuny, Robert

Martín-Belloso, Olga*

*corresponding author: omartin@tecal.udl.cat

Affiliations:

Department of Food Technology

University of Lleida – Agrotecnio Centre

Av. Alcalde Rovira Roure 191

25198, Lleida, Spain

ACCEPTED MANUSCRIPT

ACCEPTED MANUSCRIPT

ABSTRACT

The formation, characterization, photo-protective properties and release profiles of folic acid-loaded nanolaminated films were investigated by UV-visible spectroscopy, FTIR, Raman and SEM microscopy. Food-grade alginate/chitosan nanolaminates were obtained by the layer-by-layer technique and folic acid (FA) was incorporated by post-diffusion. The FA concentration of loading solutions and immersion time significantly affected the FA content in nanolaminates. The maximum FA loading was reached using FA solutions at 10 mg/mL for 30 min (54.4 μg/cm^2), or 12.5 mg/mL for 120 min (≈ 70 μg/cm^2). Nanolaminates containing FA were more stable under ultraviolet light exposure than non-encapsulated FA. The rate and concentration of FA released from nanolaminates were greater at buffer pH 7 than at pH 3, which might play a key role in the delivery and bioavailability of nutraceuticals. These results provide important information for the design of nanolaminates containing hydrophilic active compounds for food applications.

KEYWORDS: edible nanolaminates, layer-by-layer, folic acid, delivery systems, controlled release, photo-protection

ACCEPTED MANUSCRIPT

1. INTRODUCTION

Folic acid, also known as vitamin B_9, is an essential component of a healthy human diet (Saini et al., 2016). This micronutrient plays a crucial co-factor role in one-carbon metabolism, participating in the formation of DNA and maintaining the rate of cell division. It has been reported that an inadequate folate status increases the risk of neural tube birth defects (such as spina bifida), megaloblastic anemia, cardiovascular diseases and some types of cancer (Jennings and Willis, 2015). Chemically, folic acid consists of a pteridine ring bound to a *para*-aminobenzoic acid with a glutamate tail. It is highly soluble in aqueous media and alkaline conditions (Matias et al., 2014). However, the photo-degradation of folic acid takes place in presence of UV radiation, leading to the molecule breakdown into a pteridine ring and a *p*-aminobenzoic acid linked to the polyglutamate tail, and these photoproducts are biologically inactive (Delchier et al., 2016). This means that the incorporation of folic acid into foodstuffs is restricted to certain applications, and generally, large concentrations have to be used in foods to assure a health-promoting effect. Therefore, the folic acid entrapment into food-grade delivery systems might be a promising alternative to improve its stability and functional performance in a wider range of food products.

Over the past few years, the layer-by-layer (LbL) assembly technique has been exploited in the pharmaceutical and biomedical sector bringing about a considerable number of applications (Boddohi et al., 2010; Hernandez-Montelongo et al., 2016). The assembly technique is a simple and cost-effective strategy to functionalize any type of substrate consisting on the alternate deposition of oppositely charged species on a charged surface (Cerqueira et al., 2014). Although the LbL method has been scarcely studied in the food sector, its application may offer several advantages. For instance, edible nanolaminates, defined as very thin coatings of food-grade materials (e.g. polysaccharides or proteins) obtained by the LbL method, can be formed onto a food surface or food contact material. Using the LbL approach, the nanolaminates properties such as thickness, water vapor resistance, oxygen barrier and mechanical properties, and surface

56 characteristics can be fine-tune by controlling the number of layers adsorbed, the type of
57 materials adsorbed, the adsorbing solution conditions, or the terminal layer composition
58 (Klitzing and Klitzing, 2006). Probably one of the most attractive features of nanolaminates for
59 their application of the food sector is their potential capability of carrying active compounds
60 including nutraceuticals, antimicrobials, antioxidants, anti-browning agents, enzymes, flavors or
61 colorants (Durán and Marcato, 2013). From a practical viewpoint, nanolaminates might be
62 applied as edible coatings to prolong the shelf life of foods (Souza et al., 2015). Alternatively,
63 conventional packaging materials can be coated by nanolaminates to modulate their
64 physicochemical and mechanical properties (Denis-Rohr et al., 2015).

65 Alginate is a copolymer of 1→4 linked *β*-D-mannuronic acid and α-L-guluronic acid residues
66 obtained from marine brown algae. In aqueous media, the carboxyl groups of alginate are
67 ionized, conferring a negative electrical charge to the polymeric chains (Draget, 2009; Pawar
68 and Edgar, 2012). Chitosan, a cationic linear polymer composed of β-(1−4)-2-acetamido-D-
69 glucose and β-(1−4)-2-amino-D-glucose units. It is the deacetylated form of chitin, which is
70 typically found in the exoskeleton of crustaceans and fungal wall cells (Shukla et al., 2013). The
71 solubility of chitosan occurs in acid media, where amino groups are protonated and the
72 polysaccharide is converted into a cationic polyelectrolyte (Rinaudo, 2006). Recent studies
73 reported the formation of food-grade nanolaminates from alginate and chitosan (Acevedo-Fani
74 et al., 2015; Carneiro-da-Cunha et al., 2010). These systems might also contain hydrophilic
75 nutraceuticals (such as folic acid), representing a promising alternative to fortify food products.

76 As far as we are concerned, there is a lack of scientific evidence about the development of
77 edible nanolaminates containing hydrophilic nutraceuticals. The assessment of the loading and
78 release processes of the entrapped substance from nanolaminates deposited on a template can
79 give a close approximation of their behavior in real foods. Therefore, the objective of this
80 research work was to form and characterize alginate-chitosan nanolaminates containing folic
81 acid and to evaluate their loading and release behavior, as well as their ability to protect the
82 vitamin from photo-degradation.

2. MATERIALS AND METHODS

2.1. Materials

Sodium alginate Manucol® DH was purchased from FMC Biopolymers Ltd. (Scotland, U.K.). According to the manufacturer, the molecular weight of alginate is between 160 and 250 kDa, whereas the ratio of mannuronic to guluronic acid (M:G) is approximately 60-70% and 30-40%, respectively. Chitosan of high molecular weight with deacetylate degree > 75%, and powdered folic acid (FA) were obtained from Sigma Aldrich (Steinheim, Germany). Lactic acid (80–90%) and sodium hydroxide (NaOH) were purchased from Sharlau Chemie (Barcelona, Spain). Sodium chloride (NaCl) was obtained from Afora (Barcelona, Spain). Film substrates, Quartz slides (Suprasil® 300) and polyethylene terephthalate (PET) sheets (6 x 2 cm) were obtained from Hellma Analytics (Müllhein, Germany) and Isovolta (Barcelona, Spain), respectively. All solutions were prepared with deionized water obtained from a Milli-Q system (18,2 mΩ, Millipore).

2.2. Preparation of polysaccharide solutions

Alginate solutions were prepared by dissolving 0.5% w/v of powdered sodium alginate in deionized water overnight to ensure complete hindrance. Chitosan, at 0.5% w/v was dissolved in lactic acid solution (1% v/v) by stirring overnight. Then, both polysaccharide solutions were mixed with the amount of NaCl required to reach a concentration of 0.2 M. Finally, the amount of lactic acid (80-90%) or NaOH (1M) necessary to adjust the pH of alginate and chitosan to 5 and 4 was added to the solutions. These parameters were set out from preliminary experiments that proved the successful formation of nanolaminates by electrostatic interactions. Rinse solutions consisted of 0.2 M NaCl solutions at pH 5 (for alginate) or 4 (for chitosan).

2.3. Alginate-chitosan nanolaminates buildup

First, the surface of PET sheets and quartz slides was positively charged by aminolysis, following the procedure described in a previous work (Acevedo-Fani et al., 2015). For the layer-

by-layer buildup, positively charged substrates were firstly dipped in anionic alginate solution for 10 min. This was followed by two washing steps with water for 2 min, to remove the excess of unbound polysaccharide chains. The pH and ionic strength of washing solutions matched with the previous polysaccharide solution. Negatively charged substrates were further submerged in cationic chitosan solutions for 10 min, and then washed twice with water at the same solution conditions of the previous polysaccharide. All solutions remained under agitation at 30 rpm. This procedure was repeated alternating the polysaccharides deposition to a final number of 20 layers. The resulting nanolaminates were then dried at room temperature (25ºC) and stored in a desiccator with silica.

The buildup of alginate-chitosan layers in quartz slides was monitored using a V-670 UV-visible-NIR spectrophotometer (Jasco Corporation, Tokyo, Japan) containing a film holder accessory (FLH-740, Jasco Corporation, Tokyo, Japan). Absorbance spectra of quartz slides were collected after deposition of a pair of layers. Infrared spectroscopy (FTIR) was used to assess the presence of alginate and chitosan functional groups in the coated PET sheets. Spectra were collected on a FT/IR-6600 spectrophotometer (Jasco Corporation, Tokyo, Japan) fitted with an ATR cell. All measurements were performed in triplicate.

2.4. Loading of folic acid to nanolaminates

The FA loading into nanolaminates was performed using the post-diffusion method, as described in a previous study for drug loading in layer-by-layer assemblies (Jiang, Bingbing Li, 2009). Through this method, small active molecules can be easily loaded within the nanolaminates by their diffusion and immobilization in the binding sites inside the structure. To study the effect of the solution concentration on the FA loaded to nanolaminates, coated quartz slides were submerged in FA solutions at different concentrations (1-12.5 mg/mL) during 30 min, and then washed with water to remove the compound excess on the surface. This fixed immersion time was selected from preliminary assays carried out for obtaining a sufficiently high FA load in the nanolaminates that would allow its quantification. Samples were dried at

room temperature. The loading process of FA to nanolaminates was confirmed by measuring the absorbance in the UV-Visible range. To determine the total FA loading, samples were sonicated in a pH 9 phosphate buffer solution for 30 min. This procedure was repeated until absorption peaks of FA disappeared from spectra. Absorbance of sonicated solutions (with the FA extracted from nanolaminates) was measured at 364 nm, and the concentration of FA was calculated from a calibration curve (0.5-10 µg/mL - R^2 0.995126). The effect of immersion time on the loading process of FA to nanolaminates was carried out dipping coated substrates in FA solutions at a fixed concentration (12.5 mg/mL) for different times (1-240 min). The FA concentration used in the loading solutions allowed a reliable vitamin quantification in all the immersion times. The total FA loading was analyzed following the above-mentioned procedure. Measurements were carried out in triplicate.

2.5. Release of folic acid from nanolaminates

The release profiles of FA from nanolaminates were assessed using a modified method previously reported by other authors (Shukla et al., 2012). Nanolaminates assembled in PET sheets (0.7 x 2 cm) were loaded in 12.5 mg/mL FA solutions for 30 min for the release experiments. Each PET sheet was immersed in 2 ml of phosphate-citrate buffer solutions at pH 3 or 7, for 7 h at 37ºC. These pH values were selected in order to mimic the alkaline and acid conditions in the gastrointestinal tract. At predetermined times, buffer solutions were removed and stored in ice under darkness for further analysis, and 2 ml of fresh buffer were added. The buffer solutions containing FA released at pH 7 were directly analyzed by UV-visible spectroscopy at 347 nm. The buffer solutions with FA released at pH 3 were adjusted to pH 7 using 1.2 ml of 1 M sodium phosphate, and absorbance was then measured at 347 nm. The FA concentration released at each time was quantified through a calibration curve of FA solutions at pH 7 (0.5-10 µg/mL - R^2 0.991046). Each sample extracted from a vial represents the FA released from nanolaminates at a particular time rather than a cumulative amount released during the entire release period. Measurements were performed in triplicate.

2.6. Photo-stability of folic acid-loaded nanolaminates

The stability of FA encapsulated into nanolaminates was evaluated under UV lighting exposure using a method previously published, with some modifications (Aceituno-Medina et al., 2015). PET sheets (0.7 x 2 cm) coated by FA-loaded nanolaminates (FA concentration ≈ 91 µg/ml) and FA solutions (91 µg/ml) at pH 9 were placed below an UV light lamp (Osram Ultra-vitalux, 300 W) for 120 min, to accelerate folic acid degradation. The distance between lamp and samples was 20.5 cm. At certain irradiation times, FA-loaded nanolaminates were taken off from the lamp and submerged in 2 ml of phosphate buffer solution pH 9. Samples were sonicated for 30 min at room temperature. Degradation of folic acid was determined by changes in absorbance spectra of FA solutions using a UV-Visible-NIR spectrophotometer (Jasco Corporation, Tokyo, Japan). Measurements were carried out in triplicate.

2.7. Microstructure

Microstructural examinations were performed using a J-6510 Scanning Electron Microscope (JEOL Ltd., Tokyo, Japan). PET sheets coated by nanolaminates were placed on aluminum stubs and treated with carbon prior to microscopic observations. Samples were analyzed with an acceleration voltage of 5 kV.

2.8. Raman Analysis

Micro-Raman determinations of powdered FA and FA-loaded nanolaminates were carried out in a Jobin-Yvon LabRam H800 system (HORIBA Scientific, Kyoto, Japan), equipped with an Olympus BXFM optical microscope (objective 50x) and a CCD detector cooled at -70 ºC. The excitation source was a diode laser at 785 nm. The focused laser beam diameter was about 2 µm and the spectral resolution 2.5 cm^{-1}. Measurements were performed in duplicate.

2.9. Statistical analysis

One-way analysis of variance (ANOVA) was performed using the statistical and graphing software SigmaPlot 11.0 Windows package (Systat software Inc.). The Holm-Sidak method was

185 applied to determine significant differences among mean values at 5% of significance level. All
186 results are presented as the average results and standard deviations.

187 3. RESULTS AND DISCUSSION

188 3.1. Alginate-chitosan nanolaminates buildup

189 The UV-visible spectra of the coated quartz slides as a function of the number of layers are
190 shown in Fig. 1. Absorbance was measured in every bilayer since chitosan has two
191 chromophore groups (*N*-acetyl-glucosamine and glucosamine residues) in the far-UV region
192 (Kumirska et al., 2010). The optical density increased with the number of assemblies,
193 suggesting that the amount of material adsorbed was proportional to the number of layers. This
194 confirmed the successful formation of alginate-chitosan nanolaminates. Interestingly, spectra
195 did not exhibit any absorption peak from the second to the eighth layer, whereas a further
196 increase in the number of layers revealed a peak at 195 nm that corresponded to *N*-acetyl-
197 glucosamine and glucosamine. It is likely that the concentration of these molecules in
198 nanolaminates was below the limit of detection in assemblies of less than twelve layers, thus
199 explaining the absence of adsorption peaks.

200 On the other hand, the formation of nanolaminates on PET sheets was also confirmed by
201 infrared spectroscopy (Fig. 2). The bands observed in PET spectra were in good agreement with
202 results previously reported by other authors, where polyesters have three intense bands (Roger
203 et al., 2010). These bands were located at 1721 cm^{-1}, 1245 cm^{-1} and 1100 cm^{-1}, owing to the
204 C=O, C-C-O and O-C-C stretching vibrations of aromatic ester groups, respectively. After
205 assembling alginate and chitosan layers on PET sheets, these bands disappeared resulting in
206 new ones mostly located at the fingerprint zone. For instance, the band at 1410 cm^{-1} corresponds
207 to the symmetric stretching vibrations of carboxyl (COO^-) groups of alginate molecules (Kumar
208 et al., 2015). Two intense bands characteristics of the skeletal vibrations of saccharine rings in
209 both chitosan and alginate molecules were observed at 1030 cm^{-1} and 1080 cm^{-1}, corresponding
210 to C-O and C-O-C asymmetric stretching vibrations, respectively (Alves et al., 2009; Lawrie et

al., 2007). Some distinctive bands of chitosan were also found in nanolaminates spectrum. Bands at 1650 cm^{-1} (N-H-C=O stretching vibrations of amide I), 1515 cm^{-1} (amide II stretching, N-H bending vibrations or symmetric NH_3^+ deformation) and 1150 cm^{-1} (asymmetric C-O-C and C-N stretching vibrations) were particular of chitosan molecules (Aston et al., 2015). Changes in the PET infrared spectra containing the alginate-chitosan assemblies indicated the surface modification of the substrate, and hence the presence of nanolaminates.

3.2. Loading capacity of folic acid in nanolaminates

The entrapment of FA molecules into nanolaminates was carried out by post-diffusion. UV-visible spectra of alginate-chitosan assemblies before and after FA entrapment are shown in Fig. 3. Inset plot presents the UV-visible spectrum of a FA solution at pH 9. Before submerging nanolaminates in FA solutions, a single absorption peak at 195 nm was observed corresponding to chitosan molecules. After FA was loaded in nanolaminates, two new absorption peaks were observed at 295 nm and 373 nm. These peaks were distinctive of the FA solution, but appeared at 283 nm and 364 nm due to the presence of the heteroaromatic pterine chromophore, as reported previously by other authors (Choy et al., 2004; Matias et al., 2014). New peaks in the spectrum indicated the presence of FA and the swift toward greater wavelength might be probably ascribed to the presence of FA aggregates formed in nanolaminates during drying (Karukstis et al., 2002). After FA loading process, nanolaminates became yellowish and this color remained even after numerous washes with water, which suggest that FA was immobilized.

The loading process of small molecules (e.g. folic acid) into layer-by-layer assemblies is governed by a number of intrinsic properties, including the degree of swelling, hydrophilic/hydrophobic balance, dissociation constants, surface charge density and pore size of nanolaminates. The properties of small molecules, such as size, charge and hydrophilicity play an important role (Burke and Barrett, 2004). In this study, incorporation of FA was performed under alkaline conditions (buffer pH 9). In this environment, free amino groups in chitosan

237 chains are less ionized (pK_a ≈ 6.3) within the nanolaminated structure, whereas the carboxyl
238 groups in alginate molecules have a strong electrical charge (pK_a ≈ 3.65). Moreover, FA
239 molecules behave as weak acids in alkaline solutions, having a negative charge (ζ-potential ≈ -
240 34 mV, pH 9). Therefore, it was postulated that the mechanism of FA loading may have been
241 governed by hydrogen bounding rather than ionic crosslinking between the active compound
242 and polysaccharide layers. In alkaline conditions, there is not sufficient electrostatic interactions
243 between cationic chitosan and anionic FA to promote ionic binding. The fact that
244 polysaccharide-based nanolaminates have a great swelling capacity play a key role in the
245 loading of small molecules induced by H-H bounds. The presence of a large hydrogen binding
246 sites in nanolaminates creates more free volume for storage. This also allow small molecules
247 moving within the structure, thus avoiding undesirable electrostatic forces and finding sites for
248 more favorable non-electrostatic interactions (Burke and Barrett, 2004). In fact, a previous study
249 have demonstrated the high swelling capacity of alginate-chitosan nanolaminates, where the
250 film thickness in wet state can be two times greater than in dried state (Caridade et al., 2013).
251 Thereby, the great loading capacity of FA in alginate-chitosan nanolaminates could be
252 associated to the high degree of swelling in aqueous solutions. In concordance with this
253 postulation, the loading mechanism of small molecules to alginate-chitosan assemblies has been
254 previously reported using hydrophilic small drug molecules (Li et al., 2014).

255 Moreover, the kinetics of FA absorption in nanolaminates were evaluated as a function of the
256 FA concentration in loading solutions as well as the immersion time (Fig. 4). The FA
257 concentration obtained after the complete extraction from nanolaminates is shown in Fig. 4A.
258 When the concentration of FA in the immersion solutions was 1 mg/mL and 2.5 mg/mL, only a
259 slight increase from 9.8 to 11.6 μg/cm^2 in the FA concentration encapsulated in nanolaminates
260 was observed. However, a logarithmic upsurge in the concentration of encapsulated FA up to
261 53.3 μg/cm^2 was found when increasing the concentration of FA to 7.5 mg/mL in immersion
262 solutions. Interestingly, when the loading process was carried out using more concentrated FA
263 solutions, the amount of FA entrapped did not increase significantly (54.4 μg/cm^2). Therefore,

the initial concentration of the immersion solution has a remarkable impact on the final amount of active ingredient immobilized within the nanolaminated structure.

The impact of increasing the immersion time in the loading capacity of nanolaminates was investigated using FA solutions with a fixed concentration (12.5 mg/mL). Results can be observed in Fig. 4B. The FA loading rate to nanolaminates exhibited a logarithmic behavior characterized by a fast rise in the FA concentration (≈ 57 μg/cm^2) during the first 30 min, and then a slow loading process reaching 70 μg/cm^2 after 120 min. The process followed a plateau until 240 min. This result indicates that the maximum loading capacity of FA to nanolaminates is achieved at 120 min.

3.3. Microstructure of nanolaminates

Changes in the morphology of alginate-chitosan assemblies incorporating FA were examined by SEM (Fig. 5). The topography dramatically changed in nanolaminates with or without FA, as shown in Fig. 5A and 5B. The surface of nanolaminates without FA exhibited a pronounced roughness, which was attributed to globular structures composed by chitosan, which was the last polysaccharide adsorbed in the nanolaminates. In addition, this surface also presents uncoated zones identified by their smoother appearance that were ascribed to the alginate layer located below the chitosan layer. Highly irregular surfaces may contribute to increase the loading of small molecules to nanolaminates, since a rough topography has greater surface area than an even one. Hence, a large surface area results in more binding sites potentially available to encapsulate small molecules (Zhang et al., 2005), such as FA. Therefore, it is likely that the microstructure of alginate-chitosan nanolaminates may have a significant contribution in the loading process of folic acid.

The initial topography of nanolaminates dramatically changed after immersion in FA solutions, becoming in a rather smooth surface (Fig. 5B). Changes in the microstructure suggested a molecular reorganization in the polysaccharide layers due to the FA binding and the film swelling during the loading process. SEM images also revealed a stratified structure in the

internal section of nanolaminates, which was much more evident FA-loaded nanolaminates (Fig. 5C and 5D). The estimated film thickness obtained was around 2.96 μm in nanolaminates without FA, whereas the incorporation of FA apparently led to a slight reduction of thickness (2.9 μm). This is reasonable considering that the overall structure of nanolaminates was more homogeneous when it contained encapsulated FA.

3.4. Raman analysis

The presence and distribution of FA along the nanolaminated structure was examined by Raman Spectroscopy and results are shown in Fig. 6A. The spectrum of alginate-chitosan nanolaminates containing FA presented a small peak at 680 nm that it was also typical in the spectrum of powdered FA. This peak was attributed to the C-N and C-C stretching vibrations of the pteridine ring and *p*-aminobenzoic acid fragment in the FA molecule, respectively (Castillo et al., 2015). Therefore, the presence of FA in alginate-chitosan assemblies could be also confirmed by this technique. The distribution of FA along the nanolaminate structure was also studied. A cross section of a PET sheet coated by 20-layer nanolaminates that contained FA was examined by Raman spectroscopy monitoring changes in the intensity peak at 680 nm (Fig. 6B). Measurements were recorded linearly from a zero point to 1000 um far. The measurement points were located in the middle of the nanolaminate area analyzed, in order to minimize the influence of PET in the spectrum. Results indicated that the intensity patterns scarcely changed, suggesting that FA was distributed homogeneously within nanolaminate in this particular section.

3.5. Photo-stability of the encapsulated folic acid

Fig. 7 shows absorbance spectra of FA in solution and encapsulated within nanolaminates after UV irradiation. Initially, FA solutions were characterized by two main narrow peaks at 283 nm and 364 nm owing to the pteridine moieties and *p*-aminobenzoic glutamate moieties. This adsorption profile partially changed after 20 min of irradiation, observing a broad peak between 310 nm and 374 nm. Moreover, the FA spectrum dramatically changed after 120 min, being the

most representative absorption peaks eliminated, and hence suggesting a chemical degradation of the vitamin. These results are in good agreement with published studies regarding the photo-stability of FA, where the vitamin was very light sensitive (Liang et al., 2013). The FA molecule is decomposed by UV light into biologically inactive products. The main photoproducts found after UV irradiation are 6-formylpterin (FPT) and pterine-6-carboxylic acid (PCA) (Off et al., 2005). FPT has adsorption peaks at 278, 310 and 365 nm, whereas PCA is identified by two peaks at 290 and 350 nm. The increasing concentration of PCA and FPT in FA solutions gives rise to wider peaks in the absorbance spectrum. On the other hand, UV-visible spectra of nanolaminates containing FA did not exhibit remarkable changes, preserving the distinctive peak of FA after being irradiated during 120 min. Therefore, it could be confirmed that FA was more stable encapsulated in alginate-chitosan assemblies than in the non-encapsulated form when it was exposed to UV lighting. This feature may be particularly important in foods fortification with FA and for the design of functional foods.

3.6. Release behavior of folic acid from nanolaminates

The FA released from nanolaminates was investigated by UV-visible spectroscopy and results are shown in Fig. 8. To assess the possible influence of pH on the vitamin release, nanolaminates were incubated under different pH conditions that would mimic those found in the gastrointestinal tract (GIT). Most nutraceuticals including FA, are mainly adsorbed in the small intestine where pH values are alkaline. However, to achieve a successful nutraceutical delivery, several hurdles along the GIT should be surpassed, such as acid pH conditions, temperature, interactions with enzymes, etc. This factors may compromise the nutraceutical stability before reaching the adsorption site where it should be eventually released. In this study, it was observed that FA could be effectively protected from photo-degradation by its entrapment into the edible nanolaminates. Therefore, it could be expected that these nanolaminated structures would also exhibit a protective effect in GIT, or that they have the ability to control FA release when the surrounding conditions change.

342 At pH 3, only 22 % of FA was released after 7 h, whereas a complete release was observed at
343 pH 7. In the latter case, the profile was characterized by a faster release of 88 % during the first
344 hour, followed by a slower release until the seventh hour of incubation. To a lesser degree,
345 release profiles at pH 3 also exhibited a fast FA release initially, and then it reached a plateau.
346 Previous findings demonstrated that changes in pH conditions have an impact on the release of
347 small molecules. The release is normally biphasic. During the first hour, an initial burst release
348 occurs driven by an excess of entrapped compound on the surface of nanolaminates. After this
349 stage, the concentration of the compound within alginate-chitosan assemblies decreases,
350 reducing the concentration gradient, and hence the FA release (Anandhakumar et al., 2016).

351 The differences observed in the rate and extent of FA released from nanolaminates might be
352 affected by the differences in folic acid solubility at the pH conditions used for this study. While
353 the vitamin is highly soluble in alkaline media (pK_a 3.46), its solubility decreases in acid
354 environments (Gazzali et al., 2016). Therefore, the results observed in the present study
355 suggested FA might be released from nanolaminates at pH 7 due to its high solubility, whereas
356 at pH 3 the vitamin was maintained in the structure regardless the incubation time, probably
357 forming insoluble complexes within the nanolaminates. In concordance with our results, it has
358 been previously described that the pH greatly affects the release of a drug (dipyridamole) loaded
359 in poly(methacrylic acid) microspheres and protected with alginate-chitosan coatings. In this
360 study, the greater drug release from the nanostructures in acid conditions was ascribed to the
361 high solubility of the compound (Li et al., 2014). Overall, these results indicate that the
362 solubility of the active substances entrapped within the nanolaminates may determine their
363 release rate, being a promising approach to control the delivery of nutraceuticals in the
364 gastrointestinal tract.

365 4. CONCLUSIONS

366 The results obtained in this work demonstrate the feasibility of alginate-chitosan nanolaminates
367 obtained by the layer-by-layer technique as delivery systems of FA. It was established that FA

ACCEPTED MANUSCRIPT

368 loading is highly dependent on the initial concentration of FA solutions as well as the
369 immersion time. The maximum loading in films was observed at 10 mg/mL FA solution and
370 after 120 min of immersion. The FA entrapment in nanolaminates could also be confirmed by
371 Raman spectroscopy and suggested a homogeneous distribution of the vitamin. Alginate-
372 chitosan nanolaminates were also able to protect FA from degradation by UV irradiation and the
373 release profiles were affected by pH conditions, showing a greater release at pH 7. This suggests
374 that FA-loaded nanolaminates might exhibit a controlled release in the gastrointestinal tract,
375 presenting a scarce release at the stomach, but a burst released in the pH conditions of the small
376 intestine, where it is supposed to be adsorbed. However, further research should be carried out
377 using *in vitro* or *in vivo* digestion models and apply nanolaminates on food matrices. The results
378 demonstrate that edible nanolaminates might be proposed as promising candidates for delivery
379 of nutraceuticals with potential applications as active edible coatings in the food sector.

380 5. ACKNOWLEDGEMENTS

381 This research was supported by the Ministerio de Ciencia e Innovación (Spain) throughout the
382 projects AGL2009-11475 and MINECO ALG2012-35635. Author Acevedo-Fani also thanks to
383 the University of Lleida for the pre-doctoral grant.

384 6. REFERENCES

385 Aceituno-Medina, M., Mendoza, S., Lagaron, J.M., López-Rubio, A., 2015. Photoprotection of
386 folic acid upon encapsulation in food-grade amaranth (Amaranthus hypochondriacus L.)
387 protein isolate – Pullulan electrospun fibers. LWT - Food Science and Technology 62,
388 970–975. doi:10.1016/j.lwt.2015.02.025

389 Acevedo-Fani, A., Salvia-Trujillo, L., Soliva-Fortuny, R., Martín-Belloso, O., 2015. Modulating
390 Biopolymer Electrical Charge to Optimize the Assembly of Edible Multilayer Nanofilms
391 by the Layer-by-Layer Technique. Biomacromolecules 16, 2895–2903.
392 doi:10.1021/acs.biomac.5b00821

393 Alves, N.M., Picart, C., Mano, J.F., 2009. Self assembling and crosslinking of polyelectrolyte
394 multilayer films of chitosan and alginate studied by QCM and IR spectroscopy.
395 Macromolecular bioscience 9, 776–85. doi:10.1002/mabi.200800336

396 Anandhakumar, S., Gokul, P., Raichur, A.M., 2016. Stimuli-responsive weak polyelectrolyte
397 multilayer films: A thin film platform for self triggered multi-drug delivery. Materials
398 Science and Engineering: C 58, 622–628. doi:10.1016/j.msec.2015.08.039

399 Aston, R., Wimalaratne, M., Brock, A., Lawrie, G., Grøndahl, L., 2015. Interactions between
400 Chitosan and Alginate Dialdehyde Biopolymers and Their Layer-by-Layer Assemblies.
401 Biomacromolecules 16, 1807–17. doi:10.1021/acs.biomac.5b00383

402 Boddohi, S., Almodóvar, J., Zhang, H., Johnson, P.A., Kipper, M.J., 2010. Layer-by-layer
403 assembly of polysaccharide-based nanostructured surfaces containing polyelectrolyte
404 complex nanoparticles. Colloids and surfaces. B, Biointerfaces 77, 60–8.
405 doi:10.1016/j.colsurfb.2010.01.006

406 Burke, S.E., Barrett, C.J., 2004. pH-Dependent Loading and Release Behavior of Small
407 Hydrophilic Molecules in Weak Polyelectrolyte Multilayer Films. Macromolecules 37,
408 5375–5384. doi:10.1021/ma049445o

409 Caridade, S.G., Monge, C., Gilde, F., Boudou, T., Mano, J.F., Picart, C., 2013. Free-standing
410 polyelectrolyte membranes made of chitosan and alginate. Biomacromolecules 14, 1653–
411 60. doi:10.1021/bm400314s

412 Carneiro-da-Cunha, M.G., Cerqueira, M.A., Souza, B.W.S., Carvalho, S., Quintas, M.A.C.C.,
413 Teixeira, J.A., Vicente, A.A., 2010. Physical and thermal properties of a chitosan/alginate
414 nanolayered PET film. Carbohydrate Polymers 82, 153–159.

415 Castillo, J.J., Rindzevicius, T., Wu, K., Rozo, C.E., Schmidt, M.S., Boisen, A., 2015. Silver-
416 capped silicon nanopillar platforms for adsorption studies of folic acid using surface
417 enhanced Raman spectroscopy and density functional theory. Journal of Raman

ACCEPTED MANUSCRIPT

418 Spectroscopy 46, 1087–1094. doi:10.1002/jrs.4734

419 Cerqueira, M.A., Pinheiro, A.C., Silva, H.D., Ramos, P.E., Azevedo, M.A., Flores-López, M.L.,
420 Rivera, M.C., Bourbon, A.I., Ramos, Ó.L., Vicente, A.A., 2014. Design of Bio-
421 nanosystems for Oral Delivery of Functional Compounds. Food Engineering Reviews 6,
422 1–19. doi:10.1007/s12393-013-9074-3

423 Choy, J.-H., Jung, J.-S., Oh, J.-M., Park, M., Jeong, J., Kang, Y.-K., Han, O.-J., 2004. Layered
424 double hydroxide as an efficient drug reservoir for folate derivatives. Biomaterials 25,
425 3059–3064. doi:10.1016/j.biomaterials.2003.09.083

426 Delchier, N., Herbig, A.-L., Rychlik, M., Renard, C.M.G.C., 2016. Folates in Fruits and
427 Vegetables: Contents, Processing, and Stability. Comprehensive Reviews in Food Science
428 and Food Safety 15, 506–528. doi:10.1111/1541-4337.12193

429 Denis-Rohr, A., Bastarrachea, L.J., Goddard, J.M., 2015. Antimicrobial efficacy of N-halamine
430 coatings prepared via dip and spray layer-by-layer deposition. Food and Bioproducts
431 Processing 96, 12–19. doi:10.1016/j.fbp.2015.06.002

432 Draget, K.I., 2009. Alginates, in: Phillips, G.O., Williams, P.A. (Eds.), Handbook of
433 Hydrocolloids. CRC Press and Woodhead Publishing, Boca ratón, FL, pp. 807–825.

434 Durán, N., Marcato, P.D., 2013. Nanobiotechnology perspectives. Role of nanotechnology in
435 the food industry: a review. International Journal of Food Science & Technology 48,
436 1127–1134. doi:10.1111/ijfs.12027

437 Gazzali, A.M., Lobry, M., Colombeau, L., Acherar, S., Azaïs, H., Mordon, S., Arnoux, P.,
438 Baros, F., Vanderesse, R., Frochot, C., 2016. Stability of folic acid under several
439 parameters. European Journal of Pharmaceutical Sciences 93, 419–430.
440 doi:10.1016/j.ejps.2016.08.045

441 Hernandez-Montelongo, J., Lucchesi, E.G., Gonzalez, I., Macedo, W.A.A., Nascimento, V.F.,
442 Moraes, A.M., Beppu, M.M., Cotta, M.A., 2016. Hyaluronan/chitosan nanofilms

ACCEPTED MANUSCRIPT

443 assembled layer-by-layer and their antibacterial effect: a study using Staphylococcus
444 aureus and Pseudomonas aeruginosa. Colloids and Surfaces B: Biointerfaces 141, 499–
445 506. doi:10.1016/j.colsurfb.2016.02.028

446 Jennings, B.A., Willis, G., 2015. How folate metabolism affects colorectal cancer development
447 and treatment; a story of heterogeneity and pleiotropy. Cancer Letters 356, 224–230.
448 doi:10.1016/j.canlet.2014.02.024

449 Jiang, Bingbing Li, B., 2009. Tunable drug loading and release from polypeptide multilayer
450 nano fi lms. International journal of nanomedicine 4, 37–54.

451 Karukstis, K.K., Perelman, L.A., Wong, W.K., 2002. Spectroscopic Characterization of Azo
452 Dye Aggregation on Dendrimer Surfaces. Langmuir 18, 10363–10371.
453 doi:10.1021/la020558f

454 Klitzing, R. V, V Klitzing, R., 2006. Internal structure of polyelectrolyte multilayer assemblies.
455 Physical chemistry chemical physics : PCCP 8, 5012–33. doi:10.1039/b607760a

456 Kumar, S., Chauhan, N., Gopal, M., Kumar, R., Dilbaghi, N., 2015. Development and
457 evaluation of alginate–chitosan nanocapsules for controlled release of acetamiprid.
458 International Journal of Biological Macromolecules 81, 631–637.
459 doi:10.1016/j.ijbiomac.2015.08.062

460 Kumirska, J., Czerwicka, M., Kaczyński, Z., Bychowska, A., Brzozowski, K., Thöming, J.,
461 Stepnowski, P., 2010. Application of Spectroscopic Methods for Structural Analysis of
462 Chitin and Chitosan. Marine Drugs 8, 1567–1636. doi:10.3390/md8051567

463 Lawrie, G., Keen, I., Drew, B., Chandler-Temple, A., Rintoul, L., Fredericks, P., Grøndahl, L.,
464 2007. Interactions between alginate and chitosan biopolymers characterized using FTIR
465 and XPS. Biomacromolecules 8, 2533–2541.

466 Li, X., Du, P., Liu, P., 2014. Layer-by-layer polyelectrolyte complex coated poly(methacrylic
467 acid) nanogels as a drug delivery system for controlled release: structural effects. RSC

ACCEPTED MANUSCRIPT

468 Adv. 4, 56323–56331. doi:10.1039/C4RA05066E

469 Liang, L., Zhang, J., Zhou, P., Subirade, M., 2013. Protective effect of ligand-binding proteins
470 against folic acid loss due to photodecomposition. Food chemistry 141, 754–61.
471 doi:10.1016/j.foodchem.2013.03.044

472 Matias, R., Ribeiro, P.R.S., Sarraguça, M.C., Lopes, J.A., 2014. A UV spectrophotometric
473 method for the determination of folic acid in pharmaceutical tablets and dissolution tests.
474 Analytical Methods 6, 3065. doi:10.1039/c3ay41874j

475 Off, M.K., Steindal, A.E., Porojnicu, A.C., Juzeniene, A., Vorobey, A., Johnsson, A., Moan, J.,
476 2005. Ultraviolet photodegradation of folic acid. Journal of photochemistry and
477 photobiology. B, Biology 80, 47–55. doi:10.1016/j.jphotobiol.2005.03.001

478 Pawar, S.N., Edgar, K.J., 2012. Alginate derivatization: A review of chemistry, properties and
479 applications. Biomaterials 33, 3279–3305.

480 Rinaudo, M., 2006. Chitin and chitosan: Properties and applications. Progress in Polymer
481 Science 31, 603–632. doi:10.1016/j.progpolymsci.2006.06.001

482 Roger, P., Renaudie, L., Le Narvor, C., Lepoittevin, B., Bech, L., Brogly, M., 2010. Surface
483 characterizations of poly(ethylene terephthalate) film modified by a carbohydrate-bearing
484 photoreactive azide group. European Polymer Journal 46, 1594–1603.
485 doi:10.1016/j.eurpolymj.2010.04.002

486 Saini, R.K., Nile, S.H., Keum, Y.-S., 2016. Folates: Chemistry, analysis, occurrence,
487 biofortification and bioavailability. Food Research International 89, 1–13.
488 doi:10.1016/j.foodres.2016.07.013

489 Shukla, A., Fang, J.C., Puranam, S., Hammond, P.T., 2012. Release of vancomycin from
490 multilayer coated absorbent gelatin sponges. Journal of controlled release : official journal
491 of the Controlled Release Society 157, 64–71. doi:10.1016/j.jconrel.2011.09.062

ACCEPTED MANUSCRIPT

492 Shukla, S.K., Mishra, A.K., Arotiba, O.A., Mamba, B.B., 2013. Chitosan-based nanomaterials:
493 A state-of-the-art review. International journal of biological macromolecules 59, 46–58.
494 doi:10.1016/j.ijbiomac.2013.04.043

495 Souza, M.P., Vaz, A.F.M., Cerqueira, M.A., Texeira, J.A., Vicente, A.A., Carneiro-da-Cunha,
496 M.G., 2015. Effect of an Edible Nanomultilayer Coating by Electrostatic Self-Assembly
497 on the Shelf Life of Fresh-Cut Mangoes. Food and Bioprocess Technology 8, 647–654.
498 doi:10.1007/s11947-014-1436-1

499 Zhang, L., Li, B., Zhi, Z., Haynie, D.T., 2005. Perturbation of Nanoscale Structure of
500 Polypeptide Multilayer Thin Films. Langmuir 21, 5439–5445. doi:10.1021/la0501381

501

ACCEPTED MANUSCRIPT

ACCEPTED MANUSCRIPT

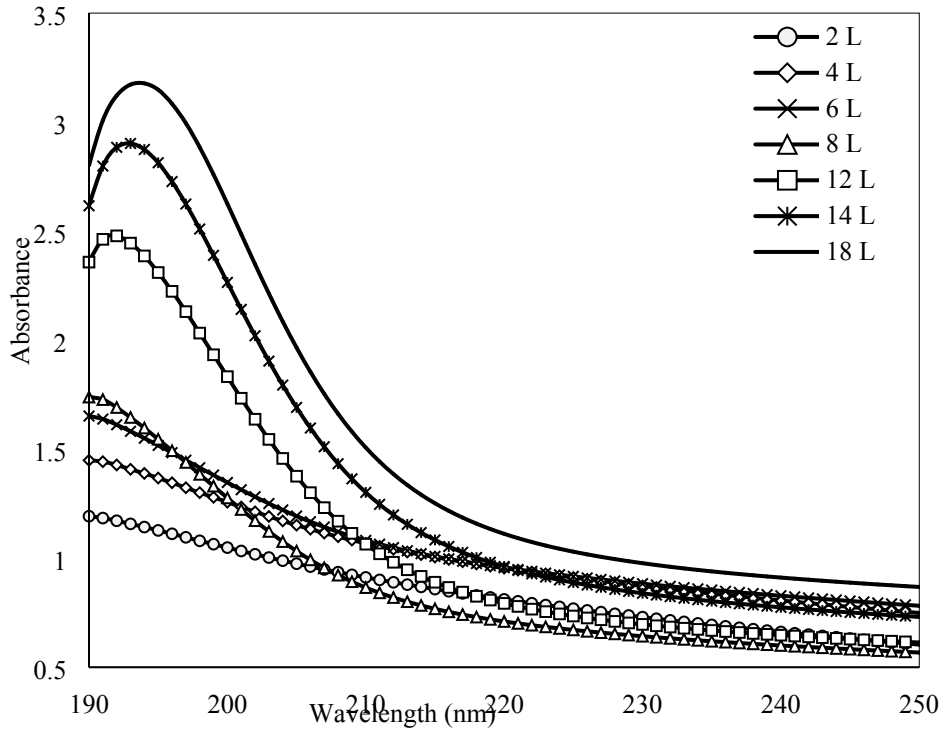

Fig. 1. UV spectra of alginate-chitosan nanolaminates as a function of the number of deposited layers (L).

ACCEPTED MANUSCRIPT

ACCEPTED MANUSCRIPT

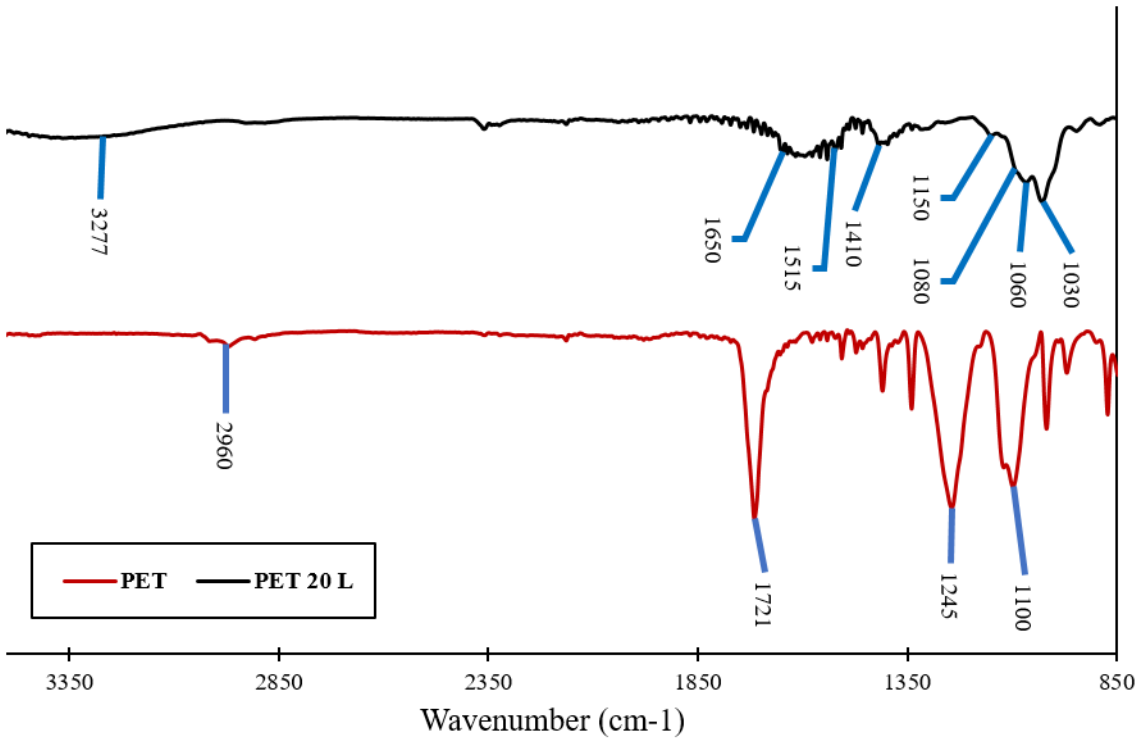

Fig. 2. Infrared spectra of bare PET sheets (PET) and PET coated by alginate-chitosan nanolaminates of 20 layers (PET 20 L).

ACCEPTED MA

ACCEPTED MANUSCRIPT

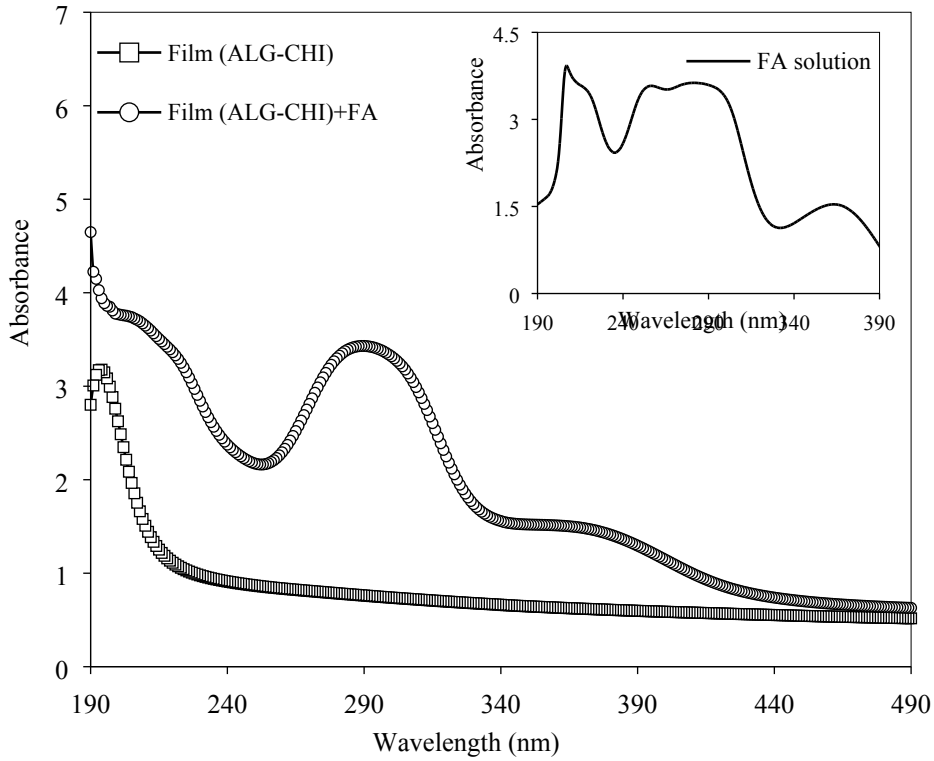

Fig. 3. UV-visible spectra of 20-layer alginate-chitosan nanolaminates before and after FA encapsulation, using loading solutions at 5 mg/mL. Inset plot corresponds to the absorbance spectrum of FA solution at pH 9.

ACCEPTED MANUSCRIPT

ACCEPTED MANUSCRIPT

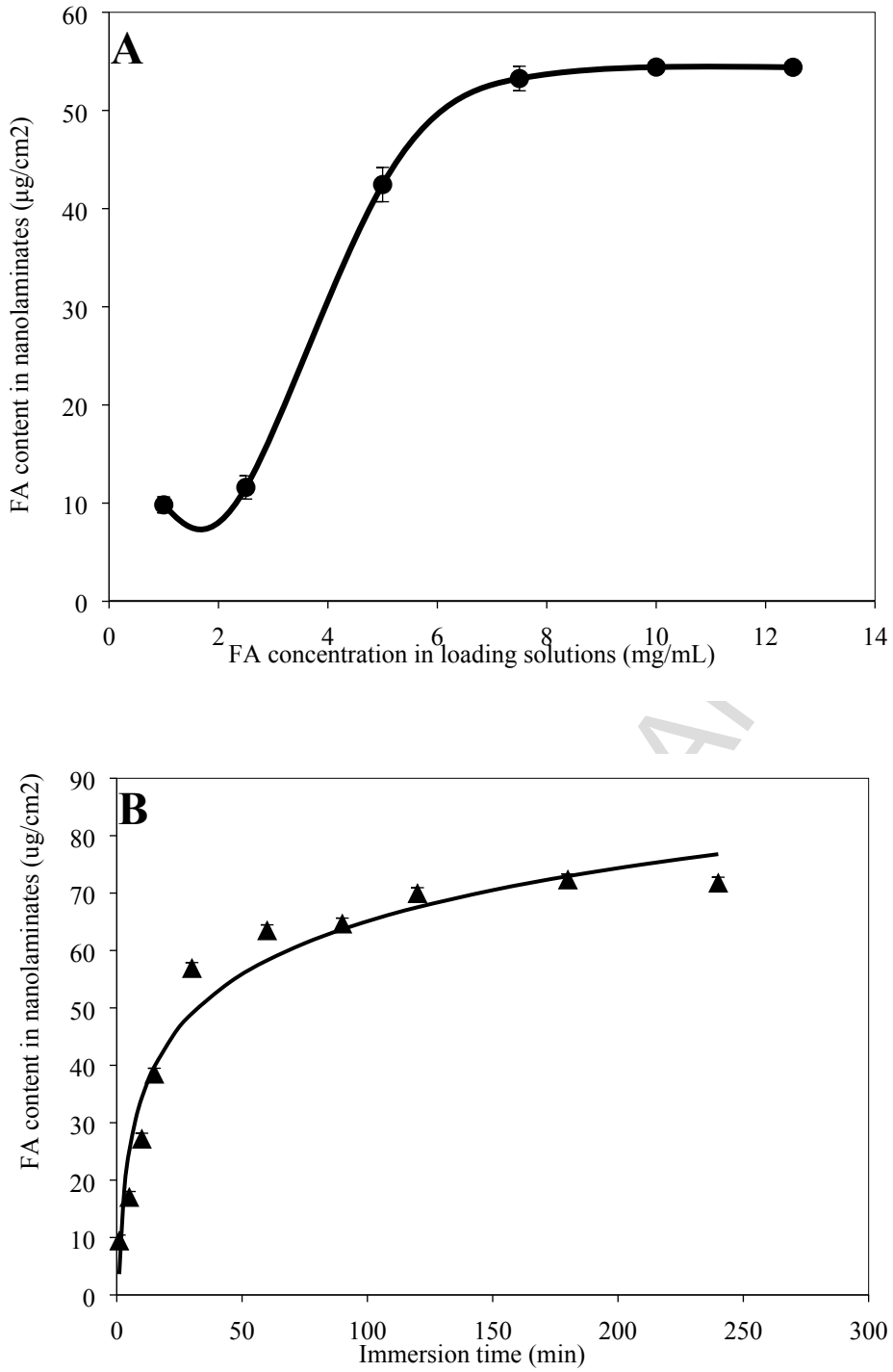

Figure 4. (A) Effect of FA concentration of the loading solutions (1-12.5 mg/mL) on the final FA content into nanolaminates. The immersion time was set to 30 min. B) Effect of the immersion time (1-240 min) on FA content within nanolaminates. The FA concentration of loading solutions was set to 12.5 mg/mL.

ACCEPTED MANUSCRIPT

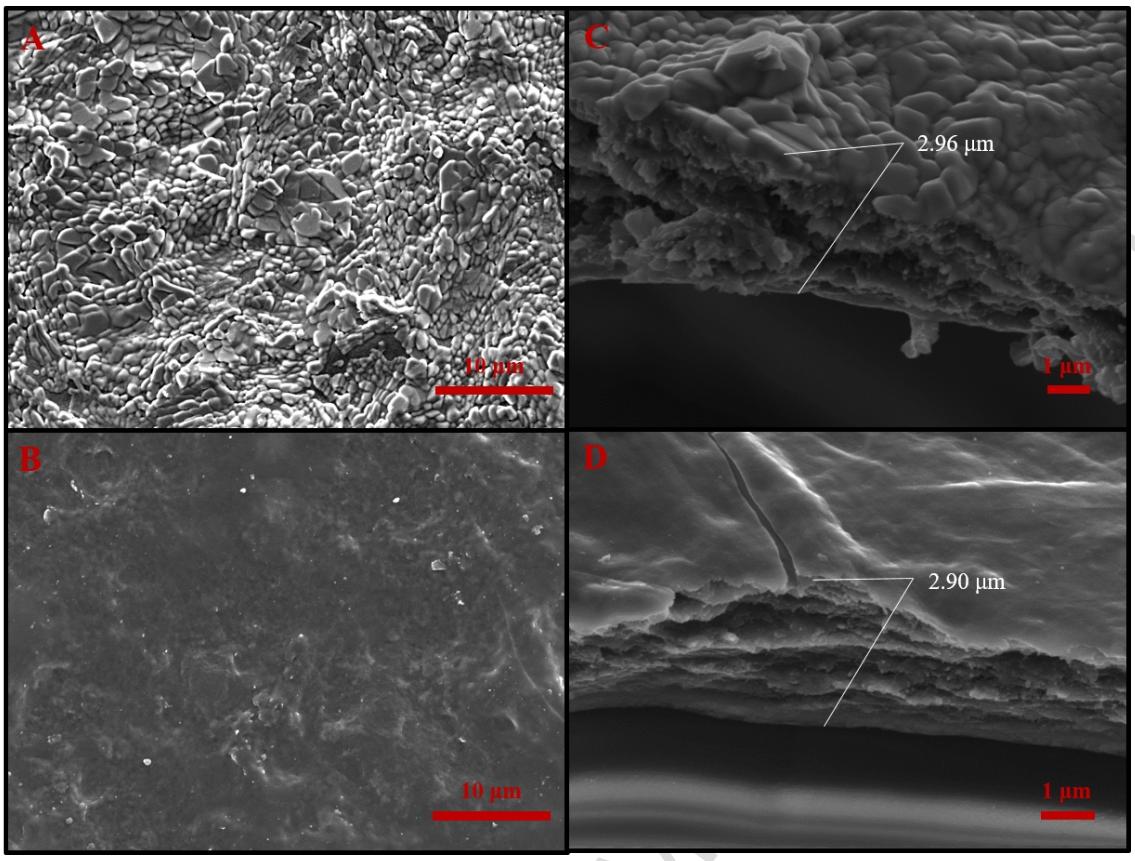

Fig. 5. A, B) Topography and C, D) cross-sectional view of alginate-chitosan nanolaminates before and after FA encapsulation.

ACCEPTED MANUSCRIPT

ACCEPTED MANUSCRIPT

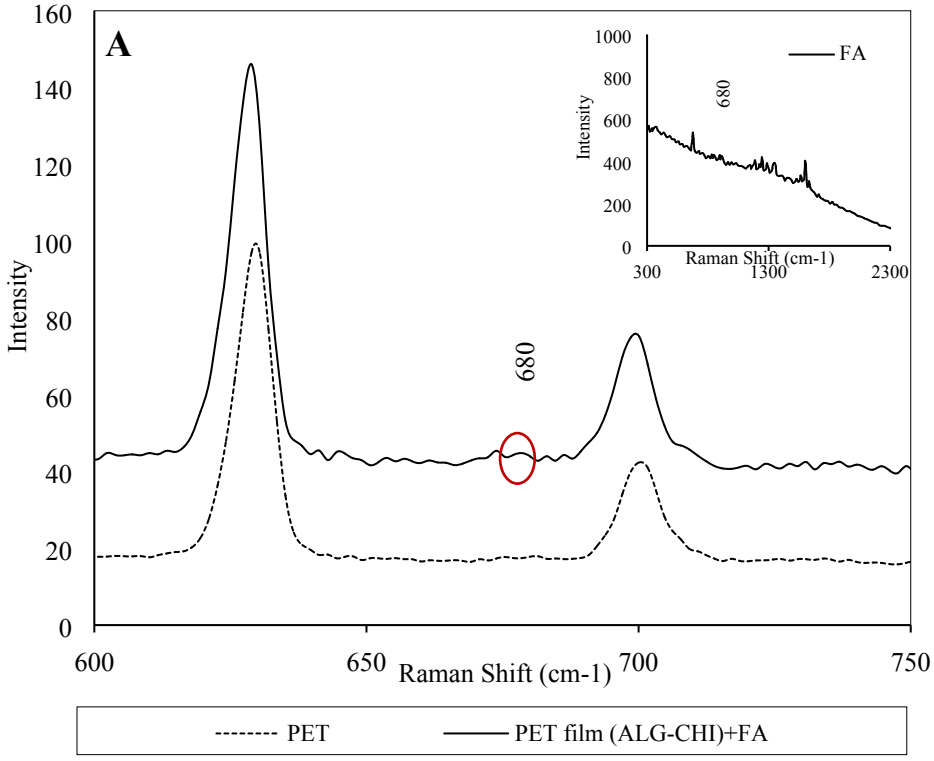

Fig. 6. A) Raman spectra of a PET sheet (PET) and PET coated by 20-layer nanolaminates containing FA. Inset plot corresponds to the Raman spectra of powdered FA. B) Changes in intensity of the FA band at 680 cm^{-1} along the cross-sectional area of nanolaminates. Inset plot indicates Raman spectra recorded in the cross-sectional area of nanolaminates at different measurement distance.

ACCEPTED MANUSCRIPT

Fig. 7. (A) Normalized absorbance spectra of folic acid (FA) solutions and (B) alginate-chitosan nanolaminates containing FA irradiated with UV-light at different exposure times (0-120 min). The FA concentration in both the solutions and the nanolaminates was 91 μg/mL.

ACCEPTED MANUSCRIPT

ACCEPTED MANUSCRIPT

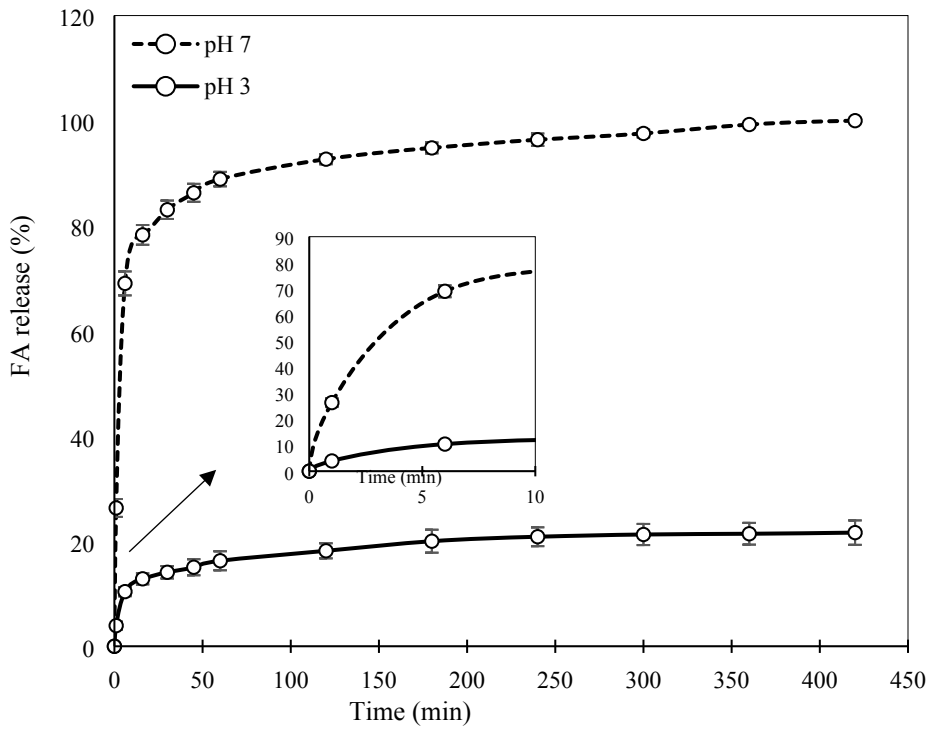

Fig. 8. Release profiles of folic acid (FA) from alginate-chitosan nanolaminates incubated at different pH conditions (pH 3 and pH 7) and 37ºC. The initial FA concentration in the nanolaminates was 91 µg/mL.

ACCEPTED MANUSCRIPT